UV completed composite Higgs model with heavy composite partners

Zi-Yu Dong,[1,2*] Cong-Sen Guan,[1,2†] Teng Ma,[3‡] Jing Shu,[1,2,4,5,6,7§] and Xiao Xue[1,2‖]

[1]*CAS Key Laboratory of Theoretical Physics, Institute of Theoretical Physics, Chinese Academy of Sciences, Beijing 100190, China*
[2]*School of Physical Sciences, University of Chinese Academy of Sciences, Beijing 100190, People's Republic of China*
[3]*Physics Department, Technion—Israel Institute of Technology, Haifa 3200003, Israel*
[4]*CAS Center for Excellence in Particle Physics, Beijing 100049, China*
[5]*School of Fundamental Physics and Mathematical Sciences, Hangzhou Institute for Advanced Study, University of Chinese Academy of Sciences, Hangzhou 310024, China*
[6]*Center for High Energy Physics, Peking University, Beijing 100871, China*
[7]*International Center for Theoretical Physics Asia-Pacific, Beijing/Hanzhou 100190, China*

(Received 15 April 2021; accepted 7 July 2021; published 16 August 2021)

We study electroweak symmetry breaking in minimal composite Higgs models $SU(4)/Sp(4)$ with purely fermionic UV completions based on a confining hypercolor gauge group and find that the extra Higgs potential from the underlying preon mass can destruct the correlation between the mass of Higgs and composite partners. Thus, the composite partners can be very heavy for successful electroweak symmetry breaking without enhancing the separation between the new physical scale and Higgs vacuum expectation value. So this kind of model can be easily realized by ordinary strong dynamics theories without artificial assumptions and, more likely, consistent with lattice simulations. The UV completion of partial compositeness predicts a light singlet Goldstone boson, which interacts with QCD and electroweak gauge bosons through Wess-Zumino-Witten terms. It can be produced through gluon fusion at LHC and decay into gauge boson pairs. We briefly discuss its phenomenology and derive its bounds from LHC searches.

DOI: 10.1103/PhysRevD.104.035013

I. INTRODUCTION

The naturalness of the Higgs potential is one of the most profound problems in particle physics. To solve this problem, new physics should be introduced to stabilize the Higgs potential. Among these new physics theories, the composite Higgs model (CHM) [1–4] is currently the most popular. In this model, the Higgs boson is a composite pseudo Nambu-Goldstone boson (PNGB), so it is insensitive to other physical scales, such as the Planck scale, and thus big hierarchy between electroweak symmetry breaking (EWSB) and the Planck scale can be achieved.

In ordinary CHMs, the Higgs potential is assumed to be only from top and gauge loop corrections. To regularize the Higgs potential and achieve a light Higgs, some composite partners should be introduced to collectively break Higgs shift symmetry or realize maximal symmetry, such as warped extra dimensions [5–7], little Higgs [4], and maximal symmetric CHMs [8,9], which results in strong correlation between the mass of Higgs and composite partners. So there always exists anomalously light top partners, around PNGB decay constant scale f, for light Higgs [10–12]. This special spectrum pattern of composite resonances, very different from QCD (the only observed strong dynamics in nature), requires some artificial ultraviolet (UV) completions. Moreover, the existing lattice simulations on some confining theories do not support this spectrum pattern [13,14], which makes constructing UV completions of ordinary CHMs very challenging.

There is the kind of CHMs that is supposed to have fermionic UV completions based on a confining hypercolor gauge group G_{HC} [15–21]. These UV completions contain two species of underlying Weyl fermions called preons, Q (QCD neutral and electroweak charged) and χ (QCD colored). The confinement of the gauge group G_{HC} will induce the spontaneously global symmetry breaking in the preon sector, generating PNGBs. The doublet PNGBs composed by Q can be treated as Higgs bosons. The colored fermionic bound states with wave function $QQ\chi$ or $Q\chi\chi$ can play the role of the top partners, which serves as

*dongziyu@mail.itp.ac.cn
†guancongsen@163.com
‡t.ma@campus.technion.ac.il
§jshu@mail.itp.ac.cn
‖xuexiao@mail.itp.ac.cn

UV completion of the partial compositeness [22]. With this setup, there are three types of CHMs with symmetric coset space in the EWSB sector: $SU(N_Q)/SO(N_Q)$, $SU(N_Q)/Sp(N_Q)$, and $SU(N_Q/2)^2/SU(N_Q/2)$ (N_Q is the number of chiral preon Q), corresponding to Q in the real, pseudoreal, and complex representations of $G_{\rm HC}$.

In this work, we study EWSB in the minimal CHMs with global symmetry breaking pattern $SU(4)/Sp(4) \cong SO(6)/SO(5)$ [16–18,20,21] in the Q sector. If preons Q are massive, the Higgs potential will get extra contributions from Q mass naturally. This extra potential can trigger EWSB in a different way together with the Higgs potential from the top and gauge sectors. Significantly, the correlation between the mass of Higgs and composite partners is lost (Higgs mass is only related to the scale difference between the partners of top and electroweak gauge bosons); thus we can get heavy composite partners (they can be as heavy as the confinement scale $\sim 4\pi f$ at the cost of more fine-tuning) and light Higgs without enhancing the separation between the Higgs vacuum expectation value (VEV) and scale f. So these kinds of CHMs with heavy fermionic and vector resonances can be easily realized by ordinary strong dynamic theories, such as $G_{\rm HC} = Sp(2N_{\rm HC})$ with $2N_{\rm HC} \leq 36$ [15], and consistent with lattice simulations, unlike ordinary CHMs.

Besides the extra single scalar η in the EWSB sector, which is extensively discussed [23–25], this model predicts another singlet PNGB σ associated with $U(1)_\sigma$ global symmetry [26], which is the subgroup of $U(1)_Q$ and $U(1)_\chi$ (overall phase of preon Q and χ). This $U(1)_\sigma$ is anomaly free under $G_{\rm HC}$, so σ can be light and crucial for testifying the partial compositeness. This singlet can interact with SM gauge fields (such as gluons) through Wess-Zumino-Witten (WZW) terms. So this singlet can be produced through gluon fusion at LHC and then decay into gauge boson pairs. We briefly discuss its phenomenology at LHC and derive its bounds for different UV completions.

The paper is organized as follows. In Sec. II, we build the concrete UV completions for CHMs based on a confining hypercolor gauge group $G_{\rm HC}$. In Sec. III, we calculate the Higgs potential from preon masses and top and gauge boson loops in two cases: ordinary and minimal maximal symmetric CHMs. In Sec. IV, we study EWSB in the Higgs potential and discuss the fine-tuning. We find that heavy top partners can be achieved. In Sec. V, we discuss the phenomenology of σ at LHC and derive its bounds. We conclude in Sec. VI. The Appendixes contain details about top partner multiplets, the form factors in the effective Lagrangian, descriptions of the gauge sector, and the mass of QCD neutral and QCD colored PNGBs.

II. THE MODEL

The consistent UV completions of CHMs with partial compositeness are limited [15] if some consistent conditions are imposed, such as asymptotic freedom and free of anomalies. In this work, we study the CHM with global symmetry breaking pattern $SU(N_Q)/Sp(N_Q)$ in the Q sector and $SU(N_\chi)/SO(N_\chi)$ in the χ sector. The global symmetry breaking pattern can thus determine that the hypercolor group in the UV completion can only be $G_{\rm HC} = Sp(2N_{\rm HC})$ with $2N_{\rm HC} \leq 36$ or $G_{\rm HC} = SO(N_{\rm HC})$ with $N_{\rm HC} = 11, 13$ [15]. For simplicity, we focus on the minimal case, where $N_Q = 4$ and $N_\chi = 6$. The Standard Model (SM) custodial symmetry $SU(2)_L \times SU(2)_R \subset SU(4)$ [hypercharge is embedded in $SU(2)_R$] and QCD $SU(3)_c \subset SU(6)$ are embedded in the global symmetry as

$$SU(4) \supset SU(2)_L \otimes SU(2)_R: \mathbf{4} = (\mathbf{2},\mathbf{2}),$$
$$SU(6) \supset SU(3)_c: \mathbf{6} = \mathbf{3} \otimes \bar{\mathbf{3}}. \quad (1)$$

The details of the UV completion of this model are summarized in Table I, where we list the SM quantum numbers of the two species of chiral preons (left-handed Weyl fermion): $Q_{1,\ldots,4}, \chi_{1,\ldots,6}$. Under this underlying strong dynamics, the global symmetry is $U(1)_\chi \times SU(4) \times U(1)_Q \times SU(6)$, where $U(1)_{\chi,Q}$ is associated with the universal phase of preons χ (Q) and is broken to $Sp(4) \times SO(6)$. One subgroup of the Abelian group $U(1)_\chi \times U(1)_Q$ has an anomaly with hypercolor $G_{\rm HC}$ symmetry, and the corresponding PNGB mass is generally at the cutoff scale, whereas the PNGB associated with the anomaly-free subgroup $U(1)_\sigma$ of $U(1)_\chi \times U(1)_Q$ can be light, which is defined by the following $U(1)_\sigma$ charge assignment of the preons [26]:

$$q_Q = N_\chi T_\chi, \qquad q_\chi = -N_Q T_Q, \quad (2)$$

where $N_{Q,\chi}$ is the number of Weyl fermions Q/χ ($N_Q = 4$ and $N_\chi = 6$ in this model) and $T_{Q,\chi}$ is the Dynkin index of hypercolor gauge group representation of Q/χ. So in this model, the total number of light Nambu-Goldstone bosons (NGBs) at a lower energy scale is

$$\mathbf{26} = \mathbf{1} + \mathbf{5} + \mathbf{20}, \quad (3)$$

where $\mathbf{1}$ is from $U(1)_\sigma$ breaking, $\mathbf{5}$ from $SU(4)/Sp(4)$, and $\mathbf{20}$ from $SU(6)/SO(6)$. Before identifying the quantum

TABLE I. Quantum numbers of the Weyl preons under the gauge group $G_{\rm HC} \times SU(3)_c \times SU(2)_L \times U(1)_Y$ and global symmetry $U(1)_\sigma$. The hypercharge is $Y = T_R^3 + X$ where X is embedded in the unbroken $SO(6)$ with $X = \mathrm{diag}\{2/3, 2/3, 2/3, -2/3, -2/3, -2/3\}$. F, A, and spin mean fundamental, two-index antisymmetric, and spinorial representation of $G_{\rm HC}$, respectively.

	$\mathrm{Sp(2N_{HC})/SO(N_{HC})}$	$\mathrm{SU(3)_c}$	$SU(2)_L \times SU(2)_R$	$\mathrm{U(1)_\sigma}$
$Q_{1,\ldots,4}$	F/spin	1	$(2,1) \oplus (1,2)$	q_Q
$\chi_{1,\ldots,6}$	A/F	$3 \oplus \bar{3}$	1	q_χ

number of these NGBs, we should choose consistent condensations of the underlying preons. Since the condensations in the Q (χ) sector are in the antisymmetric (symmetric) representation of global symmetry $SU(4)$ [$SU(6)$], we can choose the condensation of Q and χ to be SM gauge invariant [27],

$$\Sigma_{Q0} = \begin{pmatrix} i\sigma_2 & 0 \\ 0 & -i\sigma_2 \end{pmatrix}, \qquad \Sigma_{\chi 0} = \begin{pmatrix} 0 & 1_{3\times 3} \\ 1_{3\times 3} & 0 \end{pmatrix}, \tag{4}$$

which will break the global $SU(4)\times U(1)_\sigma$ to $Sp(4)$ in the electroweak sector and $SU(6)\times U(1)_\sigma$ to $SO(6)$ in the χ sector. So the quantum number of the NGBs under $SU(3)_c \times SU(2)_L \times SU(2)_R \times U(1)_X$ is

$$\begin{aligned} SU(4)/Sp(4)&: \pi_Q = (1,2,2)_0 + (1,1,1)_0, \\ U(1)_\sigma&: \ \sigma = (1,1,1)_0, \\ SU(6)/SO(6)&: \pi_\chi = (8,1,1)_0 + (6,1,1)_{\frac{4}{3}} + (\bar{6},1,1)_{-\frac{4}{3}}, \end{aligned} \tag{5}$$

where the subscript represents $U(1)_X$ charge assignment. $U(1)_X$ is the subgroup of $SO(6)$ with embedding $X = \mathrm{diag}\{2/3, 2/3, 2/3, -2/3, -2/3, -2/3\}$ and the hypercharge is defined as $Y = T_R^3 + X$ where T_R^3 is the third generator of $SU(2)_R$. Since $SU(4)/Sp(4)$ and $SU(6)/SO(6)$ are symmetric coset spaces, we can define its automorphism map

$$T \to -VT^TV^T \Rightarrow U \to VU^*V^T, \tag{6}$$

where T is the broken generators in $SU(4)/Sp(4)$ or $SU(6)/SO(6)$ coset space, and V is the VEV of $SU(4)/Sp(4)$ or $SU(6)/SO(6)$. U is the Goldstone matrix fields for $SU(4)/Sp(4)$ or $SU(6)/SO(6)$. So the linearly realized sigma field Σ and its transformation under global $SU(N)$ symmetry is

$$\Sigma \equiv UVU^T = U^2V \Rightarrow \Sigma \to g\Sigma g^T, \qquad g \in SU(N). \tag{7}$$

The linearly realized sigma in our model can be parametrized as

$$U_{Q,\chi} = e^{i\Pi_{Q,\chi}}, \qquad \Sigma_{Q,\chi} = U_{Q,\chi}^2 \Sigma_{Q0,\chi 0}, \tag{8}$$

$$\begin{aligned} \Pi_Q &= \cos\phi \frac{\sigma}{2f_Q} \mathbb{1}_4 + \frac{\sqrt{2}\pi_Q^{\hat{a}}}{f} T^{\hat{a}}, \\ \Pi_\chi &= \sin\phi \frac{\sigma}{\sqrt{6}f_\chi} \mathbb{1}_6 + \frac{\sqrt{2}\pi_\chi^{\hat{A}}}{f_6} T^{\hat{A}}, \end{aligned} \tag{9}$$

where $f_{Q,\chi}, f$, and f_6 are the decay constants of the Goldstone bosons associated with $U(1)_{Q,\chi}$, $SU(4)/Sp(4)$, and $SU(6)/SO(6)$, and $T^{\hat{a},\hat{A}}$ are the $SU(4)/Sp(4)$ [$SU(6)/SO(6)$] broken generators with normalization $\mathrm{Tr}[T^aT^b] = \delta^{ab}/2$. ϕ parametrizes the direction of the anomaly-free $U(1)_\sigma$ subgroup of $U(1)_Q \times U(1)_\chi$, with value $\tan\phi \equiv f_\chi q_\chi/(f_Q q_Q)$ [28]. Generally, the $U(1)_{Q,\chi}$ broken scale $f_{Q,\chi}$ and $SU(4)$ [$SU(6)$] broken scale are determined by the underlying dynamics. In the above Goldstone matrix, for simplicity, we can choose proper $U(1)_{Q,\chi}$ charge assignment of the underlying preons to fix $f_{Q,\chi}$ as in the following:

$$f_Q = f, \qquad f_\chi = f_6. \tag{10}$$

Notice that this choice does not affect EWSB and the relevant phenomenology. Next, we will focus on the electroweak sector. The Goldstone bosons associated with $SU(4)/Sp(4)$ can be identified as a Higgs doublet H and an extra single η,

$$(1,2,2)_0 \oplus (1,1,1)_0 = H \oplus \eta. \tag{11}$$

After EWSB, only the physical Higgs h and singlet η remains, so, in the unitary gauge, the explicit form of the Goldstone matrix is (since single σ is neutral under SM gauge interactions, we can neglect it for simplicity)

$$U_Q = \begin{pmatrix} (c' + i\frac{\eta}{\pi_Q}s')\mathbb{1}_2 & i\sigma_2 \frac{h}{\pi_Q}s' \\ i\sigma_2 \frac{h}{\pi_Q}s' & (c' - i\frac{\eta}{\pi_Q}s')\mathbb{1}_2 \end{pmatrix}, \tag{12}$$

where $\pi_Q = \sqrt{h^2+\eta^2}$, $c' = \cos(\pi_Q/(2f))$, and $s' = \sin(\pi_Q/(2f))$, and σ_2 is the second Pauli matrix.

The covariant kinetic term for these PNGBs is

$$\mathcal{L}_g = \frac{f^2}{8}\mathrm{Tr}[(D_\mu \Sigma_Q)^\dagger D^\mu \Sigma_Q], \tag{13}$$

from which we can extract the mass of W boson if Higgs acquires a VEV (the gauge interactions preserve η shift symmetry so the VEV of singlet η does not affect EWSB and, in the rest of this paper, we always assume its VEV is zero)

$$m_W^2 = \frac{1}{4}g^2 f^2 \sin^2\frac{\langle h\rangle}{f}. \tag{14}$$

So we can find the relation between the EWSB scale and global symmetry breaking scale f,

$$\xi \equiv s_h^2 = \frac{v_{\mathrm{SM}}^2}{f^2}, \qquad v_{\mathrm{SM}} = 246\ \mathrm{GeV}, \tag{15}$$

where $s_h \equiv \sin(\langle h\rangle/f)$.

In this work, we only focus on the EWSB in this minimal CHM and its relevant phenomenology. Since the colored PNGBs in the χ sector can be heavy enough to escape experimental search without affecting EWSB, which are

extensively discussed in [27], we will not discuss them in the main text (more details about these colored PNGBs are shown in Appendix E).

III. HIGGS POTENTIAL

In this section, we analyze the Higgs potential and EWSB based on the above UV completion. In CHMs, the potential of PNGBs is generated by interaction terms that explicitly break global symmetry. In ordinary CHMs, it is expected that the SM gauge interaction and top Yukawa couplings are the primary sources contributing to PNGB potential. However, we can introduce another vital contribution from the preon's mass terms to PNGB potential in this model. This contribution will bring significant modifications to the PNGB Higgs potential.

We want to emphasize again that, since the PNGB η and σ are electroweak (EW) singlets, their VEV does not affect EWSB. Moreover, we will see that the quadratic terms of their potential can be easily kept positive without fine-tuning. So without loss of generality, we always choose $\langle\eta\rangle = 0$ and $\langle\sigma\rangle = 0$ in the following discussions.

A. PNGB potential from preon mass terms

In this model, the underlying preons can be massive, which will result in the PNGBs potential, like quark masses in QCD. In this subsection, we will discuss the contributions of the mass of preon Q to the Higgs potential. The most general gauge invariant mass terms of preon Q that preserve custodial symmetry are given by

$$\mathcal{L}_{\text{mass}} = Q_i^T \Sigma_{m_Q}^{ij} Q_j + \text{H.c.}, \tag{16}$$

where Σ_{m_Q} is the mass matrix,

$$\Sigma_{m_Q} = \begin{pmatrix} im_{Q_1}\sigma_2 & 0 \\ 0 & -im_{Q_2}\sigma_2 \end{pmatrix}. \tag{17}$$

This mass matrix transforms under global symmetry $SU(4)$ as

$$\Sigma_{m_Q} \to g_Q^* \Sigma_{m_Q} g_Q^\dagger, \tag{18}$$

where g_Q is the $SU(4)$ element. According to global symmetry of the mass terms, the PNGBs potential generated by preon masses can be obtained by

$$\begin{aligned} V_m &= -C_Q f^3 \text{Tr}[\Sigma_{m_Q}.\Sigma_Q] + \text{H.c.} \\ &= 8C_Q m_Q f^3 \cos\left(\frac{\sigma\cos\phi}{f}\right)\cos\left(\frac{\pi_Q}{f}\right) \\ &\quad - 8C_Q \Delta_{m_Q} f^3 \frac{\eta}{\pi_Q}\sin\frac{\sigma\cos\phi}{f}\sin\frac{\pi_Q}{f}, \end{aligned} \tag{19}$$

where we have defined

$$m_Q = \frac{m_{Q_1} + m_{Q_2}}{2}, \qquad \Delta_{m_Q} = \frac{m_{Q_1} - m_{Q_2}}{2}. \tag{20}$$

Notice that $C_Q \sim \langle QQ\rangle/(16\pi^2 f^3)$ is an unknown form factor determined by underlying hypercolor dynamics [16], which can be positive or negative. Generally, besides its potential from Q masses, the potential of singlet σ can also be from the mass of χ; more details can be found in Appendix D.

B. PNGB potential from fermion loops

As in ordinary CHMs, the PNGB Higgs potential can also get contributions from the top loop. In this model, the UV completion constrains the top partners to be in the **6** or **10** or **1** representation of $SU(4)$. Their wave functions and quantum number under $SU(4) \times SU(6)$ are

$$\begin{aligned} &\psi_1 = \chi QQ \in (6,6), \qquad \psi_2 = \chi\bar{Q}\,\bar{Q} \in (\bar{6},6), \\ &\psi_3 = Q\bar{\chi}\,\bar{Q} \in (1,\bar{6}), \qquad \psi_4 = Q\bar{\chi}\,\bar{Q} \in (15,\bar{6}). \end{aligned} \tag{21}$$

Notice that, since composite partner ψ_3 is a global $SU(4)$ singlet, it cannot mix with the top doublet. For the most general case, top fields can mix with the other three top partner multiplets at the same time. However, in this work, since we focus on the Higgs potential and these kinds of mixings do not change the basic property of the PNGB Higgs potential, we work on the case where top quarks only mix with one multiplet of top partners through some specific dynamics, so the shift symmetry of σ is always unbroken in this case [29]. In the following discussions, we only focus on the simplest case in which the top quark only mixes with top partners in the **6** representation of $SU(4)$. Actually, the top quark singlet t_R can mix with the top partners in two ways: one is that t_R is embedded in the **6** representation of global $SU(4)$ to mix with the operator ψ_1; the other is that t_R is a global $SU(4)$ singlet and directly mixes with the $Sp(4)$ singlet component of ψ_1. These two cases can result in two different types of the Higgs potential if maximal symmetry (MS) exists in the composite sector (corresponding to ordinary MS and minimal MS cases, respectively) [30]. In the rest of this subsection, we will discuss these two cases.

1. Ordinary maximal symmetry

The left-handed fermionic operators ψ_1 can be decomposed under unbroken subgroup $Sp(4)\times SU(3)_c \times U(1)_X$ as

$$\begin{aligned} (6,6) &= (5,3,2/3) + (5,\bar{3},-2/3) \\ &\quad + (1,3,2/3) + (1,\bar{3},-2/3) \\ &\equiv \Psi_{5L} + \Psi_{5R}^c + \Psi_{1L} + \Psi_{1R}^c, \end{aligned} \tag{22}$$

where the superscript c represents charge conjugation. The contents of these multiplets can be found in Appendix A.

In order to mix with these partners, top doublet and singlet, q_L and t_R, should be embedded in **6** of $SU(4)$ and the embeddings can be chosen as

$$\Psi_{q_L} = \frac{1}{\sqrt{2}}\begin{pmatrix} 0 & Q_{q_L} \\ -Q_{q_L}^T & 0 \end{pmatrix}, \qquad Q_{q_L} = \begin{pmatrix} t_L & 0 \\ b_L & 0 \end{pmatrix},$$
$$\Psi_{t_R}^c = \frac{t_R^c}{2}\begin{pmatrix} -i\sigma_2 & 0 \\ 0 & i\sigma_2 \end{pmatrix}, \tag{23}$$

where t_R^c is written in the left-handed form. Notice that the η shift symmetry is unbroken under these top embeddings. According to the transformation properties of the fields, the most general mixing terms between the SM fermions and the top partners' invariant under $SU(4)$ global symmetry can be obtained

$$\begin{aligned}\mathcal{L}_{\rm mix} = &-\lambda_L f \mathrm{Tr}[\Psi_{q_L} U_Q (\Psi_{5R}^c + \epsilon_L \Psi_{1R}^c) U_Q^T] \\ &- \lambda_R f \mathrm{Tr}[\Psi_{t_R}^c U_Q (\Psi_{5L} + \epsilon_R \Psi_{1L}) U_Q^T] \\ &- M_5 \mathrm{Tr}[\Psi_{5L}\Sigma_{Q0}\Psi_{5R}^c\Sigma_{Q0}] \\ &- M_1 \mathrm{Tr}[\Psi_{1L}\Sigma_{Q0}\Psi_{1R}^c\Sigma_{Q0}] + \mathrm{H.c.},\end{aligned} \tag{24}$$

where $\epsilon_{L,R}$ parametrizes the mixing strength between top partner multiplet Ψ_1^c (Ψ_1) with elementary top fields. To reduce the fine-tuning in the Higgs potential for successful EWSB, the Higgs potential should be finite. To achieve this, we can assume that there is a global symmetry $SU(4)$ MS, which is different from Higgs shift symmetry in the composite sector by the following requirements:

$$\epsilon_{L,R} = 1, \qquad M \equiv M_1 = M_5. \tag{25}$$

Under this condition, we can get the ordinary maximal symmetric model, similar to [8,9]. After integrating out the heavy top partners, we can get the top quark effective Lagrangian with the simplest form,

$$\begin{aligned}\mathcal{L}_{\rm eff} = &\Pi_0^q(p)\mathrm{Tr}[\bar{\Psi}_{q_L}\not{p}\Psi_{q_L}] + \Pi_0^t(p)\mathrm{Tr}[\bar{\Psi}_{t_R}^c\not{p}\Psi_{t_R}^c] \\ &+ M_1^t(p)\mathrm{Tr}[\Psi_{q_L}\Sigma_Q^*\Psi_{t_R}^c\Sigma_Q^*] + \mathrm{H.c.},\end{aligned} \tag{26}$$

where $\Pi_0^{q,t}$ and M_1^t are form factors and their expressions can be found in Appendix A. As discussed in [8,9], we can find that the maximal symmetry can eliminate the Higgs-dependent effective kinetic terms of top quarks in the lower energy effective Lagrangian and only the effective top Yukawa is dependent on Higgs. Since the effective top Yukawa is collectively generated, $M_1^t \sim \lambda_L\lambda_R f^2 M$, and the leading Higgs potential is proportional to the top Yukawa coupling square, the Higgs potential must be finite. The top mass is easily obtained,

$$m_t = \frac{\lambda_L\lambda_R f^2 M}{\sqrt{2}M_{T_1}M_{T_2}}\sin\frac{2\langle h\rangle}{f}, \tag{27}$$

where M_{T_1} and M_{T_2} are the top partners' mass and their full expressions are listed in Appendix A.

Now, with this effective Lagrangian, we can calculate the Coleman-Weinberg potential of Higgs at one-loop level with the form

$$V_t(h) = -2N_c\int\frac{d^4p_E}{(2\pi)^4}\log\left(1 + \frac{|M_1^t|^2}{2p_E^2\Pi_0^q\Pi_0^t}\frac{h^2}{\pi_Q^2}\sin^2\frac{2\pi_Q}{f}\right). \tag{28}$$

We can expand $V_t(h)$ in top Yukawa coupling y_t up to $\mathcal{O}(y_t^2)$,

$$V_t(h) \simeq \gamma_f\left(-\sin^2\frac{\pi_Q}{f} + \sin^4\frac{\pi_Q}{f}\right)\frac{h^2}{\pi_Q^2}, \tag{29}$$

where

$$\gamma_f = 4N_c\int\frac{d^4p_E}{(2\pi)^4}\frac{|M_1^t|^2}{p_E^2\Pi_0^q\Pi_0^t}. \tag{30}$$

It is easy to find that the Higgs potential in the top sector is equivalent to the Higgs potential in ordinary maximal symmetry and the Higgs VEV naturally lies at $\xi = 1/2$.

2. Minimal maximal symmetry

In this case, t_R^c is a global $SU(4)$ singlet and thus can only mix with top partner singlet Ψ_1 directly without dressing the nonlinear PNGB matrix U_Q (η shift symmetry is still unbroken). The interactions between top fields and top partners can be expressed as

$$\begin{aligned}\mathcal{L}_{\rm mix} = &-\lambda_L f \mathrm{Tr}[\Psi_{q_L} U_Q (\Psi_{5R}^c + \epsilon_L \Psi_{1R}^c) U_Q^T] \\ &- \lambda_R f t_R^c \mathrm{Tr}[\Psi_{1L}\Sigma_{Q0}] - M_5\mathrm{Tr}[\Psi_{5L}\Sigma_{Q0}\Psi_{5R}^c\Sigma_{Q0}] \\ &- M_1\mathrm{Tr}[\Psi_{1L}\Sigma_{Q0}\Psi_{1R}^c\Sigma_{Q0}] + \mathrm{H.c.}\end{aligned} \tag{31}$$

To achieve the finite Higgs potential from the above interactions, we impose MS in the $\Psi_{5,1}$ sector again by the conditions in Eq. (25). After integrating out these heavy partners, the lower energy effective Lagrangian can be obtained,

$$\begin{aligned}\mathcal{L}_{\rm eff} = &\Pi_0^q(p)\mathrm{Tr}[\bar{\Psi}_{q_L}\not{p}\Psi_{q_L}] + \Pi_0^t(p)\bar{t}_R^c\not{p}t_R^c \\ &+ M_1^t(p)\mathrm{Tr}[\Psi_{q_L}\Sigma_Q^*]t_R^c + \mathrm{H.c.}\end{aligned} \tag{32}$$

The explicit expressions of these form factors can be found in Appendix A. The top mass can be extracted,

$$m_t = \frac{\sqrt{2}\lambda_L\lambda_R f^2 M}{M_{T_1}M_{T_2}}\sin\frac{\langle h\rangle}{f}. \tag{33}$$

The Higgs potential from the top loop is given by

$$V_f = -2N_c \int \frac{d^4p_E}{(2\pi)^4} \log\left(1 + \frac{2|M_1^t|^2}{p_E^2 \Pi_0^t \Pi_0^q} \frac{h^2}{\pi_Q^2} \sin^2\frac{\pi_Q}{f}\right). \quad (34)$$

In the limit of $\sin(\pi_Q/f) \ll 1$, the Higgs potential can be expanded up to quartic order in $\sin(\pi_Q/f)$,

$$V_f \simeq -\gamma_f \frac{h^2}{\pi_Q^2} \sin^2\frac{\pi_Q}{f} + \beta_f \frac{h^4}{\pi_Q^4} \sin^4\frac{\pi_Q}{f}, \quad (35)$$

with

$$\gamma_f = 2N_c \int \frac{d^4p_E}{(2\pi)^4} \frac{2|M_1^t|^2}{p_E^2 \Pi_0^q \Pi_0^t},$$
$$\beta_f = N_c \int \frac{d^4p_E}{(2\pi)^4} \left(\frac{2|M_1^t|^2}{p_E^2 \Pi_0^q \Pi_0^t}\right)^2.$$

C. Higgs potential in the gauge sector

As for other CHMs, the elementary EW gauge bosons interact with PNGBs through their mixing with composite vector mesons. According to the UV completion, the preons can be confined to form vector mesons with wave function and quantum number under $Sp(4)$ as

$$\rho_\mu^a \sim Q^c T^a \sigma^\mu Q : \mathbf{10}, \quad a_\mu^{\hat{a}} \sim Q^c T^{\hat{a}} \sigma^\mu Q : \mathbf{5}, \quad (36)$$

where $T^{\hat{a}}$ (T^a) is (un)broken generators of $SU(4)$. These mesons' interactions with the EW gauge boson can be determined by hidden local symmetry (more details can be seen in Appendix B). The effective Lagrangian of the EW gauge boson can be obtained by integrating out these vector mesons,

$$\mathcal{L}^{\text{eff}} = \frac{P_t^{\mu\nu}}{2}\left(g^2\Pi_0^W W_\mu^a W_\nu^a + g'^2 \Pi_0^B B_\mu B_\nu + g^2\Pi_1 \frac{h^2}{\pi_Q^2}\frac{\sin^2\frac{\pi_Q}{f}}{4}(W_\mu^1 W_\nu^1 + W_\mu^2 W_\nu^2) + \Pi_1 \frac{h^2}{\pi_Q^2}\frac{\sin^2\frac{\pi_Q}{f}}{4}(g'B_\mu - gW_\mu^3)(g'B_\nu - gW_\nu^3)\right),$$

where $P_t^{\mu\nu} = g^{\mu\nu} - p^\mu p^\nu/p^2$ is the transverse projector and the explicit expression of form factors $\Pi_0^{W,B}$ and Π_1 is shown in Appendix B. Using the full one-loop Higgs potential in Eq. (B6), we can get the leading Higgs potential by expanding it up to $\sin^2(\pi_Q/f)$ [higher power terms in $\sin^2(\pi_Q/f)$ are suppressed by gauge coupling, compared with the Higgs potential in the top sector],

$$V_g \simeq \gamma_g \frac{h^2}{\pi_Q^2} \sin^2\frac{\pi_Q}{f}, \quad (37)$$

with

$$\gamma_g = \frac{3}{8(4\pi)^2} \int dp_E^2 p_E^2 \left[\left(\frac{3}{\Pi_0^W} + \frac{1}{\Pi_0^B}\right)\Pi_1\right].$$

As in QCD, the Higgs potential correction contributed by the gauge boson loop automatically satisfies Weinberg sum rules for CHMs with fermionic UV completion. So the Higgs potential is finite and the leading order of the Higgs potential from electroweak gauge boson loops after imposing Weinberg sum rules is [10,20]

$$V_g \simeq \frac{3f^2(3g^2 + g'^2)m_\rho^2 \ln 2}{64\pi^2} \frac{h^2}{\pi_Q^2} \sin^2\frac{\pi_Q}{f}, \quad (38)$$

where, for simplicity, we require the scale f_ρ associated with these vector mesons to be equal to f, $f_\rho = f$.

IV. ANALYSIS OF THE HIGGS POTENTIAL

In this section, we will discuss EWSB, the spectrum of new fields, and fine-tuning in the Higgs potential. We will find that the Higgs potential from preon Q mass can weaken the correlation between Higgs mass and top partner mass. So in the CHMs with massive underlying preons, the composite partners can be as heavy as cutoff scale $\sim 4\pi f$ for successful EWSB.

A. EWSB in Higgs potential

The total Higgs potential that determines the EWSB vacuum can be expressed as

$$V(h) = -\gamma s_h^2 + \beta_f s_h^4 + \gamma_m c_h, \quad (39)$$

where $c_h \equiv \cos(\langle h\rangle/f)$, $s_h \equiv \sin(\langle h\rangle/f)$, $\gamma \equiv \gamma_f - \gamma_g$, and $\gamma_m \equiv 8C_m m_Q f^3$ parametrizes the Higgs potential from preon masses. In the ordinary MS case, $\beta_f = \gamma_f$. Notice that we always assume that the VEV of singlet σ and η is zero for simplicity, so the terms in the PNGB potential proportional to η and σ cannot affect Higgs VEV and can be eliminated. We will find that this condition can be easily satisfied without fine-tuning. The minimum of the potential that can realize EWSB vacuum is one of the roots of the following equation:

$$\gamma_m + 2c_h[\gamma - 2\beta_f \xi] = 0. \quad (40)$$

If $\beta_f \xi \ll \gamma$, the Higgs vacuum can be estimated as

$$c_h \approx -\frac{\gamma_m}{2\gamma} \Rightarrow \xi \approx \frac{4\gamma^2 - \gamma_m^2}{4\gamma^2}. \tag{41}$$

From this expression, we can find that, different from ordinary CHMs, the EWSB can also be triggered by preon mass contributions. The Higgs mass can be extracted from the Higgs potential,

$$m_h^2 = \frac{2\xi[\gamma + 2(2-3\xi)\beta_f]}{f^2}. \tag{42}$$

Compared with ordinary CHMs, the Higgs mass contains an extra factor γ ($m_h^2 = 8\xi\beta_f/f^2$ in ordinary CHMs). If some cancellation is imposed between γ and β_f, we can thus easily get the light Higgs and heavy composite partners simultaneously (generally, γ and β_f can have opposite sign and are independent). However, in ordinary CHMs, since the Higgs mass is only proportional to β_f, the Higgs mass is strongly correlated with the top partner mass, and there is no space to tune the parameters to achieve light Higgs and heavy partners simultaneously [10,11]. So the extra Higgs potential from preon masses can weaken the correlation between the Higgs mass and partner mass, which can be explicitly seen in the next subsection. In our model, the η potential is only from the preon mass sector (the gauge and top sector preserve η and σ shift symmetry), and after EWSB its mass can be expressed as (for $\xi \ll 1$)

$$m_\eta^2 \simeq \frac{f^2 m_h^2 - 8\xi\beta_f}{f^2\xi}. \tag{43}$$

Since β_f is positive, to prevent η from getting a VEV, β_f should satisfy the upper limit of $\beta_f < f^2 m_h^2/(8\xi)$, which will impose an upper bound on top partner mass. However, η can obtain extra mass terms from some interactions that only explicitly break η shift symmetry so the top partners can be very heavy without violating η mass bounds (more details can be seen in Appendix C). Notice that, for simplicity, we assume $\Delta_{m_Q} = 0$ such that there is no mixing between η and σ.

The singlet σ both contains the freedoms of underlying preon Q and χ, and its mass can be from both Q and χ sectors [26]. In the Q sector, its mass is only from the mass of preon Q and can be easily extracted in the EWSB phase,

$$m_\sigma^Q = m_\eta\sqrt{(1-\xi)}\cos\phi. \tag{44}$$

Its mass from the χ sector is also generated via the mass of preon χ (gauge interactions also preserve σ shift symmetry in the χ sector). More details about its mass can be seen in Appendix D. In the rest of this section, we will numerically calculate the spectrum of the new fields and fine-tuning of the Higgs potential in two different models.

B. Ordinary maximal symmetry

In an ordinary MS model, according to the analytical expressions of the Higgs potential in Eqs. (30) and (38), the Higgs potentials from the top and gauge sectors are sensitive to the composite partners mass and can be generally parametrized as

$$\gamma_f = \beta_f \simeq c_f \frac{N_c y_t^2 f^2 M_f^2}{8\pi^2}, \qquad \gamma_g \simeq c_g \frac{3g^2 m_\rho^2 f^2}{16\pi^2}, \tag{45}$$

where y_t is the top Yukawa coupling, $c_{f,g}$ is an order one positive parameter, whose analytical expressions can be derived in Eqs. (30) and (38), and M_f is the top partner mass scale. As discussed above, the correlation between Higgs and top partner mass is weakened by the extra Higgs potential from the preon mass. Substitute these expressions into the Higgs mass in Eq. (42), and we can see that the Higgs mass is sensitive to the difference between the mass scale of top and gauge bosons partners,

$$m_h^2 \sim (5c_f M_f^2 - c_g m_\rho^2)\xi. \tag{46}$$

Since $c_{f,g}$ are positive, the light Higgs indicates that the scale difference between M_f and m_ρ is small, while the mass of each composite partner can be very heavy without increasing the scale f, just at the cost of increasing fine-tuning. In ordinary CHMs, the Higgs mass is proportional to the mass scale of top partners, $m_h^2 \sim M_f^2\xi$, so the top partners should be light for light Higgs, around $M_f \approx f$, no matter how the parameters are tuned if ξ is fixed. For example, in ordinary CHMs based on deconstruction, the maximal value of lightest top partner mass is around 1.5 TeV for $\xi = 0.1$ and $m_h = 125$ GeV [11]. While, in our models, the mass of the lightest top partner can be as heavy as the cutoff ($\sim 4\pi f$) for the same benchmark point if the singlet η can acquire extra mass through some hidden interactions that only explicitly break its shift symmetry, as shown in Appendix C. As discussed in Sec. IV A, if the η potential is only from the preon mass, η mass is correlated with the top partners' mass, which imposes the upper bound on top partners. For example, if $\xi = 0.05$ and $m_\eta^2 > 0$, using the expressions in Eq. (45), top partner mass M_f should satisfy

$$M_f \lesssim \frac{\pi m_h}{y_t\sqrt{c_f N_c \xi}} \sim 1.6 \text{ TeV}. \tag{47}$$

Next, we will discuss the fine-tuning in the Higgs potential. Following the convention in [31], the fine-tuning can be quantified as

$$\Delta = \max\{\Delta_i\}, \quad \text{with} \quad \Delta_i = \left|\frac{\partial \ln \xi}{\partial \ln x_i}\right|, \tag{48}$$

where x_i is the free parameter of the model. Using the equation of the Higgs vacuum in Eq. (40), we can get the analytical expression of Δ_i,

$$\Delta_i = \frac{2x_i}{m_h^2 f^2}\left[\sqrt{1-\xi}\frac{\partial \gamma_m}{\partial x_i} + 2(1-\xi)\left(\frac{\partial \gamma}{\partial x_i} - 2\xi\frac{\partial \beta_f}{\partial x_i}\right)\right]. \quad (49)$$

If $\xi\beta_f \ll \gamma$, according to the approximate expression of ξ in Eq. (41), to get small ξ the main tuning is from the cancellation between γ_m and γ, which can be expressed as

$$\Delta_m = \frac{2\gamma_m^2}{4\gamma^2 - \gamma_m^2} = \frac{2}{\xi}(1-\xi). \quad (50)$$

Under this condition, the tuning is always minimal, even $\gamma_f \gg \beta_f$. However $\gamma_f \gg \beta_f$ always results in double tuning $\Delta \approx \gamma_f/(\xi\beta_f) \gg 1/\xi$ in ordinary CHMs. So the preon mass can relax double tuning in ordinary CHMs. In general, the tuning is mainly from the cancellations among the Higgs potential from preon mass, gauge, and top sector. The tuning from these three sectors has the same behavior and is almost at the same order of magnitude. We can explicitly look at the tuning from ρ meson mass through Eq. (49),

$$\Delta_\rho = \left|\frac{\partial \ln \xi}{\partial \ln m_\rho}\right| = \frac{8(1-\xi)\gamma_g}{m_h^2 f^2} \sim \frac{m_\rho^2}{m_h^2}. \quad (51)$$

If we choose $m_\rho = 3$ TeV and fix $\xi = 0.05$, we find $\Delta_\rho \sim 20$. Similar to other CHMs, the tuning increases as the mass of composite partners increases. This is because the Higgs potential is sensitive to the partner mass scale. To get light Higgs, more precise cancellation among $\gamma_{f,g}$ and β_f is needed if their masses are increased.

Finally, we use the measurement of fine-tuning in Eq. (48) to do the numerical calculations for the following two cases. One is the minimal case where η mass is only from the preon mass sector. In this case, its mass is related to the Higgs mass and top partners' mass scale in the EWSB phase. The other one is that its mass can also be from a hidden sector, as shown in Appendix C, so η mass can decouple with physics in EWSB. In Fig. 1, we show the fine-tuning as the function of resonance mass for the minimal (left) and nonminimal (right) case with $\xi = 0.05$, $m_h = 125$ GeV, and $m_t \in [140, 160]$ GeV. In the minimal case, since η suffers from stringent bounds from Higgs decay [32], we require $m_\eta > m_h/2$ in the numerical scan for consistency. Comparing with the nonminimal case, we can find that, in the minimal case, the bounds of η impose an upper limit on lightest top partner mass M [see Eq. (47)], which also imposes an upper limit on m_ρ thorough Higgs mass. Since M is around scale f, the tuning is minimal ($\sim 1/\xi$). In the nonminimal case, where m_η is not related to M, as discussed before, these composite partners can be as heavy as possible for successful EWSB, and the tuning increases as these partners become heavy. These numerical results confirm the above analysis.

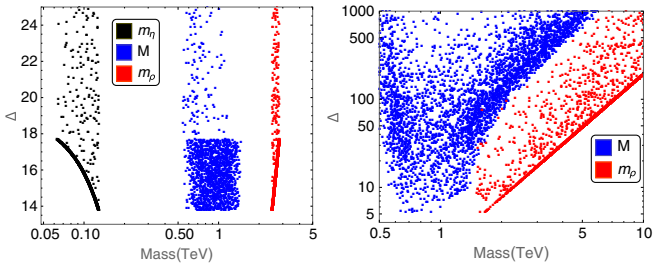

FIG. 1. Scatter plot of the tuning Δ in the model with ordinary maximal symmetry as function of mass of η (black), lightest top partner (blue), and vector meson ρ (red) for $\xi = 0.05$, $m_\eta > m_h/2$, $M > 0.5$ TeV, and $m_\rho > 2.5$ TeV. The Higgs mass is fixed at 125 GeV and the top mass range is $m_t \in [140, 160]$ GeV. Parameter M is the mass of the lightest top partner.

C. Minimal maximal symmetry

In the minimal MS CHMs [9], the Higgs potential from the gauge sector is the same as ordinary MS CHMs. γ_f is also sensitive to the top partner scale, whose parametrization is the same as in Eq. (45). While β_f is suppressed at $\mathcal{O}(y_t^4)$ and not sensitive to top partner mass, so Higgs mass is insensitive to M_f in this kind of model. The factor β_f can be generally parametrized as

$$\beta_f \simeq b_f \frac{N_c y_t^4 f^4}{16\pi^2} \ln \frac{M_f^2}{m_t^2}, \quad (52)$$

where b_f is just an order one constant. Since β_f is suppressed, the Higgs mass is always too light without preon mass contribution, $m_h \approx 100$ GeV for $M_f \approx 10f$. Meanwhile, since γ_f is much bigger than β_f, this model suffers from double tuning, $\Delta \gtrsim 95/\xi$ [9,33]. If the preon mass contribution to the Higgs potential is included, the Higgs quartic can be enhanced so Higgs can be heavy enough, and the fine-tuning can be suppressed (M_f can be reduced). On the other hand, according to the expression of η mass in Eq. (43) in the minimal case, m_η is not sensitive to top partner mass and is almost a constant for fixed ξ. For example, substituting the expression of β_f into Eq. (43), we can get $m_\eta \approx 380$ GeV for $\xi = 0.1$. Unlike the first model, this model can contain heavy enough η to escape the bounds without affecting top partners' mass. So the extra contribution to η mass from the hidden sector is not necessary. The behavior of the tuning is the same as the first model. The tuning is minimal for $M_f \sim f$, while it increases as M_f (m_ρ) increases [see Eq. (51)]. In Fig. 2, we numerically calculate the tuning as the function of resonance masses for $\xi = 0.1$ and $m_h = 125$ GeV, which confirms the above discussion.

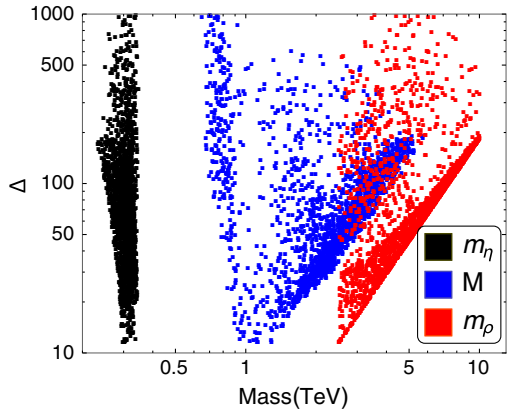

FIG. 2. Scatter plot of the tuning Δ in the minimal maximal symmetric model as function of mass of η (black), lightest top partner (blue), and vector meson ρ (red) for $\xi = 0.1$, $m_\eta > m_h/2$, $M > 0.5$ TeV, and $m_\rho > 2.5$ TeV. The Higgs mass is fixed at 125 GeV and the top mass range is $m_t \in [140, 160]$ GeV.

V. PHENOMENOLOGY AT THE LHC

If the top partners are very heavy, the first smoking gun of our model may be the presence of the extra neutral light PNGBs, especially their interactions with SM gauge bosons through WZW terms, which can give rise to very typical signatures. We expect that the σ field is the first signature of this class of CHMs, which is the main prediction of partial compositeness, because it has anomaly interactions with gluon fields, which can result in a large production cross section. The phenomenology of η is extensively discussed in [23–25]. Since its production cross section is very small, its bounds are very weak, $m_\eta > m_h/2$. We will not discuss it in this work. We will sketch the phenomenology of σ at the LHC in this section and impose some bounds to the parameter space of our model according to the LHC data. The potential of colored PNGBs can be from the gluon loop, χ mass, and top loop and is not correlated with the Higgs potential. So their mass can be at $\mathcal{O}(\text{TeV})$ for $\xi = 0.1$ without any fine-tuning and easily escape the bounds. The phenomenology of the colored PNGBs is extensively discussed in [27], so we also will not discuss it.

Generally, as discussed before, σ can acquire mass from both Q and χ mass sectors,

$$m_\sigma = m_\sigma^Q + m_\sigma^\chi, \tag{53}$$

where $m_\sigma^{Q,\chi}$ is the mass from the Q (χ) sector in Eq. (44) [Eq. (D4)]. If σ mass is only from the Q sector, it is very light (always lighter than m_η in the minimal case) and is excluded by LHC detections. To have heavy σ, its mass should be dominated by χ mass contributions in Eq. (D4). Since the gauge and top sectors preserve their shift symmetry, they do not interact with top or gauge bosons through Yukawa or gauge interactions. However, since σ is composed by both χ and Q freedoms, it mainly interacts with SM gauge fields A_μ^i through WZW terms, which can be parametrized as follows:

$$\mathcal{L}_{\text{WZW}} = \frac{g_i^2 \kappa_i}{32\pi^2 f_\sigma} \sigma \epsilon^{\mu\nu\alpha\beta} A_{\mu\nu}^i A_{\alpha\beta}^i, \tag{54}$$

where $f_\sigma \equiv \sqrt{(q_Q^2 f_Q^2 + 3 q_\chi^2 f_\chi^2/2)/(q_Q^2 + q_\chi^2)}$ is the decay constant associated with σ, and $A_{\mu\nu}^i$ generally denotes the gauge field strength of type $i = W$, B, g (EW triplet, hypercharge, gluon). The coefficients κ_i can be given by

$$\kappa_i = \frac{q_Q \kappa_i^Q + q_\chi \kappa_i^\chi}{\sqrt{q_Q^2 + q_\chi^2}}, \tag{55}$$

where $\kappa_i^{Q,\chi}$ only depends on the coset space of the Q and χ condensates and, for our case, we have

$$\kappa_W^Q = \kappa_B^Q = d_Q, \qquad \kappa_g^\chi = 2 d_\chi, \qquad \kappa_B^\chi = 12 X^2 d_\chi, \tag{56}$$

where d_Q/d_χ are the dimensions of hypercolor representation of Q/χ and X is the $U(1)$ hypercharge defined in Table I. The main production channel for the σ field is through gluon-gluon fusion and the cross section at the proton-proton center-of-mass frame can be parametrized by the partial decay width and the parton luminosities,

$$\sigma(pp \to \sigma) = \frac{1}{m_\sigma s} C_{gg} \Gamma(\sigma \to gg), \tag{57}$$

where $\Gamma(\sigma \to gg)$ is its decay width to gluon pairs, s is the center-of-mass energy square, and the dimensionless partonic integral C_{gg} is

$$C_{gg} = \frac{\pi^2}{8} \int_{m_\sigma^2/s}^1 \frac{dx}{x} g(x) g\left(\frac{m_\sigma^2}{sx}\right). \tag{58}$$

The remarkable feature here is that σ interactions with gauge fields are completely fixed by the representations of the preons under G_{HC}. So σ decay widths can reflect the physics of UV completion. The analytical formulas of the partial decay widths to the SM gauge bosons are

$$\Gamma(\sigma \to gg) = \frac{\alpha_s^2 \kappa_g^2}{8\pi^3} \frac{m_\sigma^3}{f_\sigma^2},$$

$$\Gamma(\sigma \to \gamma\gamma) = \frac{\alpha^2}{64\pi^3} (\kappa_W + \kappa_B)^2 \frac{m_\sigma^3}{f_\sigma^2},$$

$$\Gamma(\sigma \to W^+W^-) = \frac{\alpha_W^2 \kappa_W^2}{32\pi^3} \frac{m_\sigma^3}{f_\sigma^2} \left(1 - \frac{4m_W^2}{m_\sigma^2}\right)^{3/2},$$

$$\Gamma(\sigma \to ZZ) = \frac{\alpha^2}{64\pi^3 t_W^4} (\kappa_W + \kappa_B t_W^4)^2 \frac{m_\sigma^3}{f_\sigma^2} \left(1 - \frac{4m_Z^2}{m_\sigma^2}\right)^{\frac{3}{2}},$$

$$\Gamma(\sigma \to Z\gamma) = \frac{\alpha^2}{32\pi^3 t_W^2} (\kappa_W - t_W^2 \kappa_B)^2 \frac{m_\sigma^3}{f_\sigma^2} \left(1 - \frac{m_Z^2}{m_\sigma^2}\right)^3,$$

where $\alpha_W = \alpha/s_W^2$ and s_W (t_W) is the sine (tangent) function of the Weinberg angle θ_W. Taking the $\sigma \to \gamma\gamma$ decay channel as the reference channel, we can obtain the ratios of σ decay widths for $G_{\rm HC} = SO(11)$, which is only determined by the UV completion and independent of f_σ,

$$\frac{\Gamma_{gg}}{\Gamma_{\gamma\gamma}} = 870, \quad \frac{\Gamma_{WW}}{\Gamma_{\gamma\gamma}} = 4.2, \quad \frac{\Gamma_{ZZ}}{\Gamma_{\gamma\gamma}} = 0.416, \quad \frac{\Gamma_{Z\gamma}}{\Gamma_{\gamma\gamma}} = 3.1,$$

and the ratios for $G_{\rm HC} = SO(13)$,

$$\frac{\Gamma_{gg}}{\Gamma_{\gamma\gamma}} = 711, \quad \frac{\Gamma_{WW}}{\Gamma_{\gamma\gamma}} = 2.4, \quad \frac{\Gamma_{ZZ}}{\Gamma_{\gamma\gamma}} = 0.17, \quad \frac{\Gamma_{Z\gamma}}{\Gamma_{\gamma\gamma}} = 2.3.$$

For $G_{\rm HC} = Sp(2N_{\rm HC})$ with $N_{\rm HC} = 2$, the ratios are

$$\frac{\Gamma_{gg}}{\Gamma_{\gamma\gamma}} = 68399, \quad \frac{\Gamma_{WW}}{\Gamma_{\gamma\gamma}} = 713.6, \quad \frac{\Gamma_{ZZ}}{\Gamma_{\gamma\gamma}} = 144, \quad \frac{\Gamma_{Z\gamma}}{\Gamma_{\gamma\gamma}} = 206.2.$$

For the maximum situation, $N_{\rm HC} = 18$, we obtain

$$\frac{\Gamma_{gg}}{\Gamma_{\gamma\gamma}} = 76439.5, \quad \frac{\Gamma_{WW}}{\Gamma_{\gamma\gamma}} = 1179.7,$$
$$\frac{\Gamma_{ZZ}}{\Gamma_{\gamma\gamma}} = 259.8, \quad \frac{\Gamma_{Z\gamma}}{\Gamma_{\gamma\gamma}} = 282.4.$$

From the above calculations, we can explicitly see that the decay channel into gluon pairs is dominant over the other channels.

Using WZW interaction in Eq. (54), we simulate different signatures of σ in LHC from the following channels:

$$gg \to \sigma \to A^i A^j, \tag{59}$$

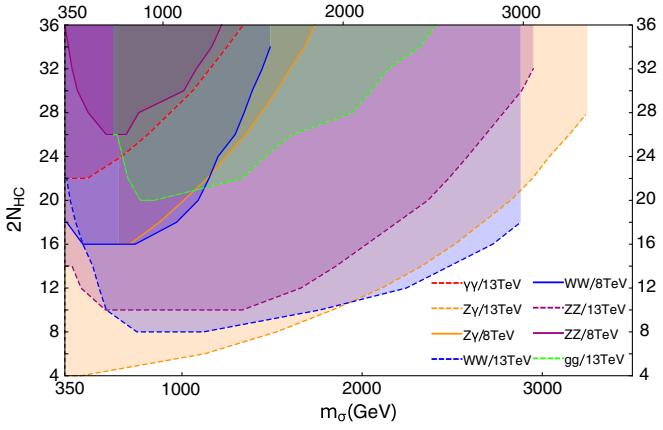

FIG. 3. Bounds from LHC detections on the mass of σ for different hypercolor group $G_{\rm HC} = Sp(2N_{\rm HC})$ with $2N_{\rm HC} \leq 36$ and decay constant fixed at $f_\sigma = 800$ GeV. The different color regions represent the excluded parameter space via σ different decay channels. The cross sections of the channels with $\gamma\gamma$ and gg final states at 8 TeV LHC are always smaller than the experimental value and thus there are no constraints on m_σ.

where $A = \{W^\pm, Z, \gamma, g\}$. By comparing with the experimental data from 8 TeV [34–38] and 13 TeV LHC [39–43], we derive the bounds of m_σ for different hypercolor groups with $f_\sigma = 800$ GeV held fixed, as shown in Fig. 3 (the color regions are excluded parameter space). For the $G_{\rm HC} = Sp(2N_{\rm HC})$ model, the bounds of σ increase as $N_{\rm HC}$ increases. For the $G_{\rm HC} = SO(11/13)$ hypercolor model, the strongest constraints come from the $Z\gamma$ decay channel and we find $m_\sigma < 2.6$ TeV is excluded for the $SO(11)$ hypercolor group and $m_\sigma < 2.8$ TeV is excluded for $SO(13)$.

VI. CONCLUSIONS

We studied the minimal composite Higgs model $SU(4)/Sp(4)$ with purely fermionic UV completions based on a confining hypercolor gauge group $G_{\rm HC}$. Under this strong dynamics, two species of underlying Weyl fermions in different representations of $G_{\rm HC}$, $Q_{1,\ldots,4}$ (QCD colorless) and $\chi_{1,\ldots,6}$ (QCD colored), should be introduced to generate the composite Higgs doublet, composed by Q alone, as well as top partners, composed by both Q and χ. Different from ordinary composite Higgs models, the Higgs potential is not only from top and gauge loop corrections but also from the masses of preon Q. With this extra contribution, electroweak symmetry breaking can be realized differently and the correlation between the mass of Higgs and top partners is weakened.

To keep the Higgs potential from the top sector finite, we impose maximal symmetry in this model. Since the maximal symmetry can be realized in two different ways, we study its EWSB in two cases, the ordinary and minimal maximal symmetric CHMs. In the first case, even the Higgs potential from the top and gauge sectors is sensitive to composite resonance mass scales; the Higgs mass is only sensitive to the difference between the mass scale of composite vector mesons and top partners. So the composite partners of top and gauge bosons can be as heavy as possible, even around the cutoff $\sim 4\pi f$, for successful EWSB just at the cost of high fine-tuning. While the top partner mass is around scale f for light Higgs in ordinary CHMs without preon mass contributions, no matter how the parameters are tuned. However, since η mass is related to the top partner mass if it is only from preon masses, positive η mass square imposes the upper bounds on the top partner mass, such as $M < 1.6$ TeV for $\xi = 0.05$ and $m_\eta^2 > 0$. But the mass of η can also be generated from the hidden interactions, which only break η shift symmetry. If this contribution is dominant in η mass, the correlation between the mass of top partners and η is destructed, and thus the composite top partners can be heavy arbitrarily (generally, it should be smaller than cutoff scale) without any constraints. In the minimal maximal symmetric case, the Higgs quartic from the top sector is suppressed at quartic order in top Yukawa coupling and is

not sensitive to the top partner scale M_f. However, without Higgs potential contributed by preon mass, the Higgs mass is always too light even M_f is around cutoff scale, which always results in double tuning $\sim 95/\xi$. While the extra Higgs potential from preon mass can enhance the Higgs quartic, the Higgs mass can be heavy enough for several TeV top partners with $\xi = 0.1$. Meanwhile, the tuning is significantly suppressed as low as minimal $\sim 1/\xi$ for $M > 1.5$ TeV. The η mass is also insensitive to M_f so it can be heavy enough to avoid the bounds $m_\eta > m_h/2$ and is almost fixed for fixed ξ if its mass is only from the preon mass sector (around 300 GeV for $\xi = 0.1$).

The partial compositeness predicts an extra $U(1)_\sigma$ PNGB σ in this model. Since it contains both the freedoms of Q and χ, it can interact with SM EW and QCD gauge bosons through Wess-Zumino-Witten terms, which are determined by UV completions. Especially, its decay branch ratio into different gauge boson pairs can reveal the UV theory. This singlet can be resonance produced through gluon fusion and decay into gauge boson pairs. This can be the typical phenomenology of this kind of model at LHC, and we derive the bounds of σ mass for different $G_{\rm HC}$ gauge groups.

ACKNOWLEDGMENTS

J. S. is supported by the National Natural Science Foundation of China (NSFC) under Grants No. 11947302, No. 11690022, No. 11851302, No. 11675243, and No. 11761141011, and by the Strategic Priority Research Program of the Chinese Academy of Sciences under Grants No. XDB21010200 and No. XDB23000000. T. M. is supported by the United States-Israel Binational Science Foundation (BSF) (NSF-BSF program Grant No. 2018683) and the Azrieli Foundation and by "Study in Israel" Fellowship for Outstanding Post-Doctoral Researchers from China and India by PBC of CHE.

APPENDIX A: TOP PARTNERS AND FORM FACTORS IN TOP EFFECTIVE LAGRANGIAN

For the top partners $\Psi_{5,1}$ in the Lagrangian (24), their explicit embeddings in representation **6** of $SU(4)$ are

$$\Psi_{5L} = \begin{pmatrix} \frac{1}{2}T_5 i\sigma^2 & \frac{1}{\sqrt{2}}Q \\ -\frac{1}{\sqrt{2}}Q^T & \frac{1}{2}T_5 i\sigma^2 \end{pmatrix}, \qquad Q = \begin{pmatrix} T & X_{5/3} \\ B & X_{2/3} \end{pmatrix},$$
$$\Psi_{1L} = \begin{pmatrix} \frac{1}{2}T_1 i\sigma^2 & 0 \\ 0 & -\frac{1}{2}T_1 i\sigma^2 \end{pmatrix},$$
$$\Psi^c_{5R} = \begin{pmatrix} \frac{1}{2}T^c_5 i\sigma^2 & \frac{1}{\sqrt{2}}Q^c \\ -\frac{1}{\sqrt{2}}Q^{cT} & \frac{1}{2}T^c_5 i\sigma^2 \end{pmatrix}, \qquad Q^c = \begin{pmatrix} -X^c_{2/3} & B^c \\ X^c_{5/3} & -T^c \end{pmatrix},$$
$$\Psi^c_1 = \begin{pmatrix} \frac{1}{2}T^c_1 i\sigma^2 & 0 \\ 0 & -\frac{1}{2}T^c_1 i\sigma^2 \end{pmatrix}. \tag{A1}$$

The form factors in Eq. (26) and masses of top partners in Eq. (27) in an ordinary maximal symmetric model can be expressed as

$$\Pi^q_0 = 1 - \frac{\lambda_L^2 f^2}{p^2 - M^2}, \quad \Pi^t_0 = 1 - \frac{\lambda_R^2 f^2}{p^2 - M^2}, \quad M^t_1 = \frac{\lambda_L \lambda_R f^2 M}{M^2 - p^2},$$
$$M_{T_1} = \sqrt{f^2\lambda_L^2 + M^2}, \quad M_{T_2} = \sqrt{f^2\lambda_R^2 + M^2}. \tag{A2}$$

The form factors in Eq. (32) and masses of top partners in Eq. (33) in the minimal maximal symmetric model can be expressed as

$$\Pi^q_0 = 1 - \frac{\lambda_L^2 f^2}{p^2 - M^2}, \quad \Pi^t_0 = 1 - \frac{4\lambda_R^2 f^2}{p^2 - M^2}, \quad M^t_1 = \frac{\lambda_L \lambda_R f^2 M}{p^2 - M^2},$$
$$M_{T_1} = \sqrt{f^2\lambda_L^2 + M^2}, \quad M_{T_2} = \sqrt{4f^2\lambda_R^2 + M^2}. \tag{A3}$$

APPENDIX B: GAUGE SECTOR

According to the hidden local symmetry, the vector resonances ρ_μ transform nonlinearly, while the axial resonances a_μ transform homogeneously, under a global $SU(4)$ transformation $\mathbf{g}$,

$$\rho_\mu = \rho^a_\mu T^a, \qquad \rho_\mu \to \mathbf{h}\rho_\mu \mathbf{h}^\dagger + \frac{i}{g_\rho}\mathbf{h}\partial_\mu \mathbf{h}^\dagger,$$
$$a_\mu = a^{\hat{a}}_\mu T^{\hat{a}}, \qquad a_\mu \to \mathbf{h} a_\mu \mathbf{h}^\dagger, \tag{B1}$$

where $\mathbf{h} = \mathbf{h}(\mathbf{g}, \pi^{\hat{a}})$ is the nonlinearly realized $Sp(4)$ element. So at leading order in derivatives, the general Lagrangian allowed by Eq. (B1) is

$$\mathcal{L}_\rho = -\frac{1}{2}\mathrm{Tr}[\rho_{\mu\nu}\rho^{\mu\nu}] + f_\rho^2 \mathrm{Tr}[(g_\rho \rho_\mu - E^a_\mu T^a)^2],$$
$$\mathcal{L}_a = -\frac{1}{2}\mathrm{Tr}[a_{\mu\nu}a^{\mu\nu}] + \frac{f_a^2}{\Delta^2}\mathrm{Tr}[(g_a a_\mu - \Delta d^{\hat{a}}_\mu T^{\hat{a}})^2], \tag{B2}$$

where $iU^\dagger D_\mu U = d^{\hat{a}}_\mu T^{\hat{a}} + E^a_\mu T^a$, $\rho_{\mu\nu} = \partial_\mu\rho_\nu - \partial_\nu\rho_\mu - ig_\rho[\rho_\mu, \rho_\nu]$, $a_{\mu\nu} = \nabla_\mu a_\nu - \nabla_\nu a_\mu$, and $\nabla_\mu = \partial_\mu - iE^a_\mu T^a$. After integrating out the heavy resonances at tree level, the $SU(4)$ invariant Lagrangian, at quadratic order in the gauge fields and in momentum space, is

$$\mathcal{L}^{\rm eff} = \frac{P_t^{\mu\nu}}{2}(\Pi_0(p^2)\mathrm{Tr}[A_\mu A_\nu] - p^2(W^a_\mu W^a_\nu + B_\mu B_\nu) + \frac{\Pi_1(p^2)}{4}\mathrm{Tr}[(A_\mu\Sigma + \Sigma A^T_\mu)(A_\nu\Sigma + \Sigma A^T_\nu)^\dagger]), \tag{B3}$$

where $A_\mu = gW^a_\mu T^a_L + g' B_\mu T^3_R$, $P_t^{\mu\nu} = g^{\mu\nu} - p^\mu p^\nu/p^2$ is the projector on transverse field configurations, and $\Pi_{0,1}$ are form factors. From the above Lagrangian, we get the

most general effective Lagrangian for gauge bosons with explicit dependence on the Higgs field,

$$\mathcal{L}^{\text{eff}} = \frac{P_t^{\mu\nu}}{2}\Big(g^2\Pi_0^W W_\mu^a W_\nu^a + g'^2\Pi_0^B B_\mu B_\nu + g^2\Pi_1\frac{h^2}{h^2+\eta^2}\frac{s^2}{4}(W_\mu^1 W_\nu^1 + W_\mu^2 W_\nu^2) + \Pi_1\frac{h^2}{h^2+\eta^2}\frac{s^2}{4}(g'B_\mu - gW_\mu^3)(g'B_\nu - gW_\nu^3)\Big),$$

where $s = \sin(\sqrt{h^2+\eta^2}/f)$,

$$\Pi_0^W = -\frac{p^2}{g^2} + p^2\frac{f_\rho^2}{p^2-m_\rho^2}, \qquad \Pi_0^B = \Pi_0^W(g\to g'),$$
$$\Pi_1 = f^2 + 2p^2\left(\frac{f_a^2}{p^2-m_a^2} - \frac{f_\rho^2}{p^2-m_\rho^2}\right). \tag{B4}$$

Here we define the mass parameters

$$m_\rho^2 = f_\rho^2 g_\rho^2, \qquad m_a^2 = \frac{f_a^2 g_a^2}{\Delta^2}. \tag{B5}$$

So it is easy to get the Higgs potential at one-loop level by integrating out the gauge fields and going to Euclidean momenta space,

$$V_g(h) = \frac{3}{2}\int\frac{d^4p_E}{(2\pi)^4}\left(2\log\left[\Pi_0^W + \Pi_1\frac{h^2}{h^2+\eta^2}\frac{s^2}{4}\right] + \log\left[\Pi_0^B\Pi_0^W + \Pi_1\frac{h^2}{h^2+\eta^2}\frac{s^2}{4}(\Pi_0^B+\Pi_0^W)\right]\right). \tag{B6}$$

APPENDIX C: A MECHANISM TO PRODUCE HEAVY η

In the gauge and top sectors, these interactions are $U(1)_\eta$ invariant, so the SM field loops do not contribute to η potential. To produce a heavy η while preserving Higgs and σ shift symmetry, we introduce an electroweak singlet complex scalar ϕ. To break η shift symmetry, we suppose it is embedded in **6** representation of $SU(4)$ in the form

$$\Phi = \frac{\phi}{2}\begin{pmatrix} i\sigma_2 & \mathbf{0} \\ \mathbf{0} & i\sigma_2 \end{pmatrix}. \tag{C1}$$

So its general couplings to the PNGBs are given by

$$\mathcal{L}_\phi = \partial_\mu\phi^\dagger\partial^\mu\phi - m_\phi^2\phi^\dagger\phi - y_\phi f^2\text{Tr}[\Phi\Sigma^\dagger]\text{Tr}[\Phi^\dagger\Sigma] = \partial_\mu\phi^\dagger\partial^\mu\phi - m_\phi^2\phi^\dagger\phi - 4y_\phi f^2\frac{\eta^2}{\pi_Q^2}\sin^2\left(\frac{\pi_Q}{f}\right)\phi^\dagger\phi. \tag{C2}$$

The PNGB potential at one-loop level is

$$V_\eta \simeq \frac{y_\phi f^2 C_\phi}{(4\pi)^2}\frac{\eta^2}{\pi_Q^2}\sin^2\left(\frac{\pi_Q}{f}\right)\Lambda_Q^2, \tag{C3}$$

where $\Lambda_Q \sim 4\pi f$ is the condensed scale of preon Q and C_ϕ is an order one constant. Generally, $y_\phi C_\phi$ can be positive so η becomes massive from the scalar loop. Its mass is naturally at $\mathcal{O}(f)$, so η can be heavy enough to survive experimental bounds without any fine-tuning.

APPENDIX D: MASS OF σ FROM χ SECTOR

The χ preon mass can explicitly break the shift symmetry of σ and thus can contribute to σ mass. The gauge invariant mass term of preon χ can be aligned with condensation $\Sigma_{\chi 0}$,

$$\mathcal{L}_{\text{mass}}^\chi = m_\chi\chi_l^T\Sigma_{\chi 0}^{lm}\chi_m + \text{H.c.}, \tag{D1}$$

where m_χ is the preon mass. The mass matrix transforms under global symmetry $SU(6)$ as

$$\Sigma_{\chi 0} \to g_\chi^*\Sigma_{\chi 0}g_\chi^\dagger, \tag{D2}$$

where $g_\chi \in SU(6)$. Similarly, σ potential from χ masses can be easily derived according to the global symmetry

$$V_m^\chi = -C_\chi f_6^3 m_\chi\text{Tr}[\Sigma_{\chi 0}.\Sigma_\chi] + \text{H.c.} = -12C_\chi m_\chi f_6^3\cos\left(\frac{2\sigma\sin\phi}{\sqrt{6}f_6}\right), \tag{D3}$$

where $C_\chi \sim \langle\chi\chi\rangle/(4\pi)^2 f_6^3$ is the form factor related to strong dynamics [16]. We can also read the σ mass from Eq. (D3),

$$m_\sigma^\chi = 2\sin\phi\sqrt{2C_\chi m_\chi f_6}. \tag{D4}$$

APPENDIX E: MASS OF COLORED PNGBs

The colored PNGBs multiplet π_8 and π_6 (π_6^c) in the **8** and **6** ($\bar{\mathbf{6}}$) representation of QCD $SU(3)_c$ can get the potential from gluon loops, the mass of preons m_χ, and top loops. However, the potential of PNGBs π_8 from the top sector is suppressed by ξ, so this kind of potential can be neglected. As discussed in [27], the mass of these PNGBs can be generally expressed as by spurionic analysis

$$m_{\pi_8}^2 = 8C_\chi m_\chi f_6 + \frac{3}{4}g_s^2 C_g f_6^2,$$
$$m_{\pi_6}^2 = 8C_\chi m_\chi f_6 + \frac{5}{6}g_s^2 C_g f_6^2 + C_{RR}\frac{f^4}{f_6^2}, \tag{E1}$$

where C_g and C_{RR} are $\mathcal{O}(1)$ form factors depending on underlying dynamics and g_s is QCD gauge coupling.

The terms proportional to m_χ, g_s^2, and C_{RR} are, respectively, the correction from the mass of χ, gluon loop, and right-handed top loop. We can find their mass is uncorrelated with Higgs mass so they can be heavy enough [$\mathcal{O}$(TeV)] without introducing EWSB fine-tuning. For example, if these form factors $C_{\chi,g,RR} > 0$, these PNGBs can be heavier than $\sqrt{C_g} f_6 \approx 1.6\,\text{TeV}$ for $\xi = 0.1$, $f_6 = f \approx 800\,\text{GeV}$, and $C_g = 4$, which is consistent with LHC bounds $m_{\pi_8,\pi_6} > 1.1$ TeV.

[1] D. B. Kaplan and H. Georgi, Phys. Lett. **136B**, 183 (1984).
[2] H. Georgi and D. B. Kaplan, Phys. Lett. **145B**, 216 (1984).
[3] M. J. Dugan, H. Georgi, and D. B. Kaplan, Nucl. Phys. **B254**, 299 (1985).
[4] N. Arkani-Hamed, A. G. Cohen, E. Katz, and A. E. Nelson, J. High Energy Phys. 07 (2002) 034; N. Arkani-Hamed, A. G. Cohen, E. Katz, A. E. Nelson, T. Gregoire, and J. G. Wacker, J. High Energy Phys. 08 (2002) 021.
[5] L. Randall and R. Sundrum, Phys. Rev. Lett. **83**, 3370 (1999).
[6] R. Contino, Y. Nomura, and A. Pomarol, Nucl. Phys. **B671**, 148 (2003).
[7] K. Agashe, R. Contino, and A. Pomarol, Nucl. Phys. **B719**, 165 (2005).
[8] C. Csaki, T. Ma, and J. Shu, Phys. Rev. Lett. **119**, 131803 (2017).
[9] C. Csáki, T. Ma, J. Shu, and J. H. Yu, Phys. Rev. Lett. **124**, 241801 (2020).
[10] D. Marzocca, M. Serone, and J. Shu, J. High Energy Phys. 08 (2012) 013.
[11] O. Matsedonskyi, G. Panico, and A. Wulzer, J. High Energy Phys. 01 (2013) 164.
[12] M. Redi and A. Tesi, J. High Energy Phys. 10 (2012) 166.
[13] Bennett, D. K. Hong, J. W. Lee, C. J. D. Lin, B. Lucini, M. Piai, and D. Vadacchino, J. High Energy Phys. 12 (2019) 053.
[14] Bennett, D. K. Hong, J. W. Lee, C. J. D. Lin, B. Lucini, M. Mesiti, M. Piai, J. Rantaharju, and D. Vadacchino, Phys. Rev. D **101**, 074516 (2020).
[15] G. Ferretti and D. Karateev, J. High Energy Phys. 03 (2014) 077.
[16] J. Galloway, J. A. Evans, M. A. Luty, and R. A. Tacchi, J. High Energy Phys. 10 (**2010**) 086.
[17] T. A. Ryttov and F. Sannino, Phys. Rev. D **78**, 115010 (2008).
[18] G. Cacciapaglia and F. Sannino, J. High Energy Phys. 04 (2014) 111.
[19] T. Ma and G. Cacciapaglia, J. High Energy Phys. 03 (2016) 211.
[20] C. Csáki, T. Ma, and J. Shu, Phys. Rev. Lett. **121**, 231801 (2018).
[21] C. S. Guan, T. Ma, and J. Shu, Phys. Rev. D **101**, 035032 (2020).
[22] D. B. Kaplan, Nucl. Phys. **B365**, 259 (1991).
[23] Y. Wu, T. Ma, B. Zhang, and G. Cacciapaglia, J. High Energy Phys. 11 (2017) 058.
[24] D. Buarque Franzosi, G. Ferretti, L. Huang, and J. Shu, SciPost Phys. **9**, 077 (2020).
[25] A. Arbey, G. Cacciapaglia, H. Cai, A. Deandrea, S. Le Corre, and F. Sannino, Phys. Rev. D **95**, 015028 (2017).
[26] A. Belyaev, G. Cacciapaglia, H. Cai, G. Ferretti, T. Flacke, A. Parolini, and H. Serodio, J. High Energy Phys. 01 (2017) 094; 12 (2017) 088(E).
[27] G. Cacciapaglia, H. Cai, A. Deandrea, T. Flacke, S. J. Lee, and A. Parolini, J. High Energy Phys. 11 (2015) 201.
[28] The other orthogonal combination of $U(1)_{Q,\chi}$ corresponds to $U(1)_{\sigma'}$, which has anomaly with $Sp(2N_{\text{HC}})$, and the associated scalar σ' can get heavy enough mass from anomaly and $Sp(2N_{\text{HC}})$ instanton effects and thus decouple from the theory at lower energy.
[29] ψ_1, ψ_2, and ψ_4 have different $U(1)_\sigma$ charges, so if the top fields couple to two of them simultaneously, the $U(1)_\sigma$ symmetry is broken and the potential of σ should be proportional to the product of their mixing couplings. If top quarks only mix with one multiplet of top partners, $U(1)_\sigma$ is always preserved, and thus top loops do not contribute to σ potential.
[30] MS is the global symmetry in the composite sector, while the preon mass terms are in the representation of global symmetry $SU(4)$ and explicitly break it. So the mass terms do not influence maximal symmetry.
[31] R. Barbieri and G. F. Giudice, Nucl. Phys. **B306**, 63 (1988).
[32] G. Aad *et al.* (ATLAS and CMS Collaborations), J. High Energy Phys. 08 (2016) 045.
[33] C. Csáki, C. S. Guan, T. Ma, and J. Shu, Phys. Rev. Lett. **124**, 251801 (2020).
[34] G. Aad *et al.* (ATLAS Collaboration), Phys. Rev. D **92**, 032004 (2015).
[35] CMS Collaboration, CMS-PAS-EXO-16-025.
[36] G. Aad *et al.* (ATLAS Collaboration), J. High Energy Phys. 01 (2016) 032.
[37] G. Aad *et al.* (ATLAS Collaboration), Eur. Phys. J. C **75**, 69 (2015).
[38] V. Khachatryan *et al.* (CMS Collaboration), Phys. Rev. D **91**, 052009 (2015).
[39] M. Aaboud *et al.* (ATLAS Collaboration), J. High Energy Phys. 03 (2018) 042.
[40] M. Aaboud *et al.* (ATLAS Collaboration), J. High Energy Phys. 03 (2018) 009.
[41] M. Aaboud *et al.* (ATLAS Collaboration), Phys. Lett. B **775**, 105 (2017).
[42] A. M. Sirunyan *et al.* (CMS Collaboration), J. High Energy Phys. 09 (2018) 148.
[43] A. M. Sirunyan *et al.* (CMS Collaboration), Phys. Lett. B **769**, 520 (2017); **772**, 882(E) (2017).